MultiCraft

International Journal of Engineering, Science and Technology
Vol. 14, No. 2, 2022, pp. 22-33

INTERNATIONAL JOURNAL OF ENGINEERING, SCIENCE AND TECHNOLOGY

www.ijest1-ng.com
www.ajol.info/index.php/ijest

Joint-design effect on the metallurgical and mechanical behavior of duplex stainless steel welds

Rajat Dhiman[1], Sorabh Singhal[2], Ravindra K. Saxena[3]

[1,2,3] *Department of Mechanical Engineering, Sant Longowal Institute of Engineering and Technology, Longowal-148106, Punjab, INDIA*
**Corresponding Author: e-mail: rksaxena04@yahoo.com, Tel+ 91 92162 20006*
ORCID iDs: http:/orcid.org/ 0000-0001-8668-2978 (Saxena)

Abstract

In the present investigation, the influence of joint design on the microstructure and the mechanical properties of SAF 2205 duplex stainless steel welds are reported. Plates with two different joint designs were welded using the gas tungsten arc welding process. To investigate the sole effect of joint design, the joints were designed in such a way that both joints have similar groove volumes. The weldments were investigated for microstructural characterization, ferrite content, and microhardness study; later, they were subjected to Charpy V-notch impact test, transverse tensile test, and fatigue testing in order to investigate the mechanical performance. Both the weld joints were able to achieve 100% joint efficiency in view of the transverse tensile test. Different weld joint configurations demonstrated the influence of the differential heat dissipation characteristics of the joints, evident from different morphological features revealed through optical microscopy of the weldment. The welding affected the ferrite(α)-austenite(γ) ratio of the weld metals and differed the welds in terms of ferrite content in the root and weld pass. The weld zone of the U-joint showed a 65.8% ferrite fraction and thus showed 18% more hardness as compared to the V-joint, while the V-joint had the highest yield stress of 617 MPa. The study revealed that the U-joint performed better in comparison to the V-joint in terms of microhardness, impact toughness, and fatigue behavior. The U-joint could resist around 15% more fatigue cycles than the V-joint under high cycle fatigue.

Keywords: Duplex stainless steel; gas tungsten arc welding (GTAW); joint design; mechanical behavior; SAF 2205.

DOI: http://dx.doi.org/10.4314/ijest.v14i2.3

Cite this article as:
Dhiman R., Singhal S., Saxena R.K. 2022. Joint-design effect on the metallurgical and mechanical behavior of duplex stainless steel welds. *International Journal of Engineering, Science and Technology*, Vol. 14, No. 2, pp. 22-33. doi: 10.4314/ijest.v14i2.3

Received: July 17, 2021; Accepted: July 28, 2022; Final acceptance in revised form: August 8, 2022

1. Introduction

Duplex stainless steels (DSS) are dual-phase steels comprising ferrite (α) and austenite (γ) phases in a balanced proportion. The balanced microstructure of the alloy provides excellent mechanical properties and good corrosion resistance when compared to ferritic or austenitic stainless steel (ASS), as reported by Gunn (1997). Because of these properties, DSSs find their applications in aggressive environments like offshore industries, food processing units, pulp industries, chemical tankers, and large structures like bridges as well, as reviewed by Jebaraj et al. (2017). The DSSs have excellent hot cracking resistance as compared to ASS due to higher ferrite content, but on some occasions, the Heat affected zone (HAZ) of DSS demonstrates loss of strength and lower corrosion resistance. Therefore, welding of DSSs is a challenging task as the material is subjected to intense localized thermal cycles during welding which disturbs the microstructural phase balance of the weldmetal Leonard et al. (2000). The studies by Koussyet al. (2004) and Lin et al. (2012) show that during the solidification of the weld metal, several secondary precipitations

(like carbides, σ, and χ-phase) take place in the temperature range of 400~1000°C. When the weldment is subjected to this temperature range, the intermetallic compounds lead the weld to embrittlement and affect the mechanical and corrosion properties of the weldment. Verma and Taiwade (2017) reviewed that welding with high energy arc process provides lower cooling and promote the formation of austenite in the weldmetal while low energy arc process like electron beam welding (EBW) and laser beam welding (LBW) can significantly reduce the austenite content of the weld metal up to around 5% due to faster cooling rate. They concluded that a lower energy arc suppresses the intermetallic precipitations.

The composition of filler metal has also a prominent effect on the resulting weld microstructure than the cooling rate, as reported by Muthupandi et al. (2003). Welding of DSSs is generally recommended with Ni-rich filler wires to promote the austenite content. Mu´nez et al. (2010) compared duplex and austenite fillers and reported a decrease in the α/γ ratio in the weld metal of the joint fabricated using austenitic filler. Moreover, Paulraj and Garg (2016) and Zhang et al. (2017) investigated that the addition of 2-5% N_2 in pure Argon (Ar) shielding reduces the amount of precipitation, increases the austenite content, and improves the toughness and corrosion resistance. The phase balance of the microstructure can be retained with the help of post-weld heat treatment (PWHT). Badji et al. (2008) found that the aging of the weldment in the temperature range of 600-1000°C records the lowest toughness values (up to 6J/cm^2) at 850°C due to the maximum amount of sigma phase (σ-phase). Zhang et al. (2012) performed the aging at 1050°C and found that the austenite content increases and a balanced state of α/γ transformation reach, which enhances the mechanical and corrosion properties of DSS welds.

The mechanical properties, like tensile strength as well as elongation characteristics, are strongly dictated by weldjoint design as reported by Luo et al. (2014) and Rahmani et al. (2014). The joint design finds application during welding of thick sections in large steel structures for example bridges and tankers etc. The joint design parameters have a profound effect on the performance and application of the weldment as studied by Jang et al. (2001). Ling et al.(2015) observed that joint configuration is an important factor in welding that critically controls the heat dissipation characteristics of the weld and affects the microstructure and the mechanical properties of the component. The investigation, carried out by Sharma and Shahi (2014), on the effect of different joint designs on quenched and tempered steel welded joints shows that joint design variation can exert a strong influence on the mechanical properties of the welds.

Researchers have made attempts to retain the phase balance of DSS weldmetal by investigating different welding techniques, varying shielding gas composition, using different fillers, and by PWHT. The joint design influences the heat input and heat dissipation characteristics in welding, which may influence the microstructure and mechanical properties of the weld Rahmani et al. (2014). It is found from the literature that no such study is available which shows the effect of joint design on the behavior of DSS weld. To bridge the gap, the present work aims to investigate the effect of two different joint configurations, viz. V-joint and U-joint, on the resulting microstructure and the mechanical properties of DSS type SAF 2205 welds.

2. Experimental procedures

2.1 Material and Welding process

Duplex stainless steel type SAF 2205 was used as the base metal and ER 2209 as the filler material. The chemical composition of the base metal and filler material is given in Table 1. Rolled plates of 12 mm thickness and 75 x 400 mm^2 in size were welded with a single V-joint and single U-joint configuration.

Table 1: The chemical composition by wt. (%) of base metal and filler material

Material	C	Mn	Si	Cr	Ni	Mo	N	S	P	Fe
Base metal	0.02	0.84	0.41	22.84	4.65	3.8	0.186	0.003	0.028	Bal.
Filler material	0.01	1.8	0.4	22.7	8.5	3.2	0.16	0.001	0.015	Bal.

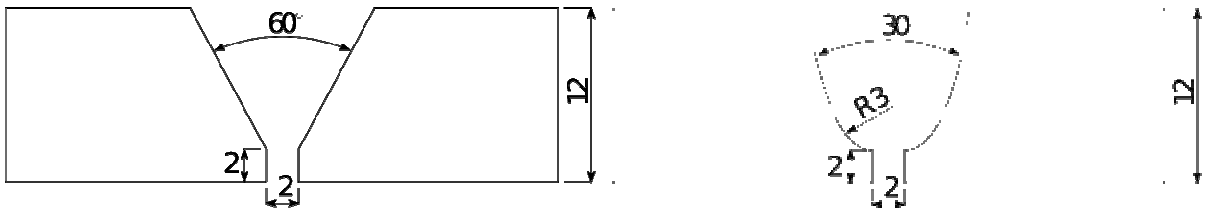

(a) (b)

Figure 1. Joint designs for welds (a) V-joint, (b) U-joint, (all dimensions are in mm)

In order to investigate the sole effect of joint design, the joints were designed in such a way that both joints have a similar cross-section area of around 55.7 mm^2. Figure 1 shows the schematic of both the joint configurations used in the study. Before the start of the welding, plates were properly cleaned to remove oil and dirt. To remove any oxide scale formation and heat tint, stainless steel wire brush was used. Welding was performed using the gas tungsten arc welding (GTAW) process using pure argon (Ar) as

shielding gas (AWS 2004). The inter-pass temperature of 120 ^{o}C was kept using external flame heating to maintain a uniform cooling rate and to avoid the coarsening of HAZ grains. The welding was performed by a certified welder and the process parameters were determined based on initial trial runs. The process parameters used for welding are listed in Table 2.

Table 2: Process parameters in welding

Weldment	No. of passes	Current (A)	Voltage (V)	Velocity (mm/sec)	Average heat input (kJ/mm)
V-Joint	8	140-170	13	0.9-3.3	0.67
U-Joint	7	140-170	13	1.0-2.4	0.55

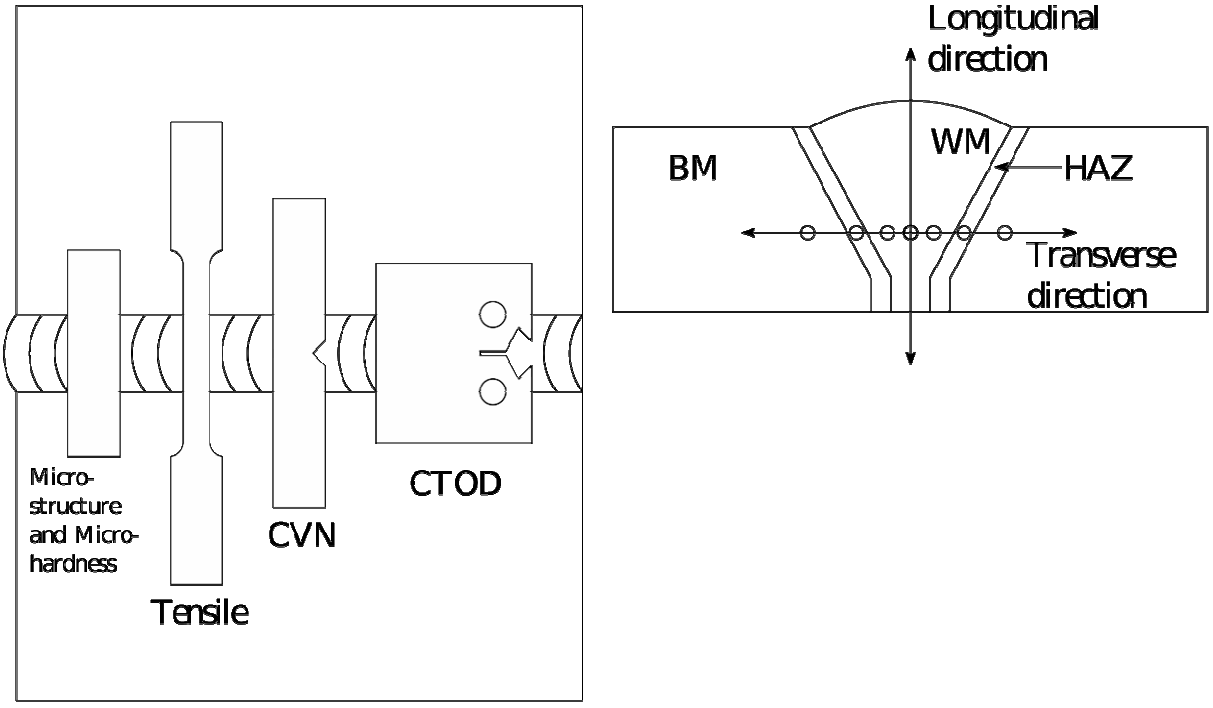

(a) (b)

Figure 2(a) Schematic of the specimen extraction plan, (b) Ferrite and microhardness measurementpoints

2.2 Metallurgical testing

The schematic of the extraction plan of the specimens used for metallurgical and mechanical investigations is shown in Fig.2a. The specimens from both welds were mechanically polished and etched with modified Beraha's etchant, containing 1.5g $K_2S_2O_5$, 100ml HCL, 15g NH_4HF_2 and 100 ml distilled water, by immersion for 8 sec for microstructural characterization. The microscopic investigation was conducted using an optical microscope coupled with a CCD camera to capture the micrographs.

The ferrite content measurement was carried out in different zones of a weld. Hosseini et al. (2018) and Putz et al. (2019) compared a number of methods viz. image analysis with light optical metallography, magnetic measurements with Ferit scope and Magne-Gage, and X-ray diffractometry (XRD), used for the measurement of ferrite content in DSS. They found that Feritscope underestimates the ferrite measurement by a factor of 1.1but still it finds extensive application due to ease in application. In the present work, Ferrite content was measured in different zones of weldments by using Fischer's Feritscope. The measurements were taken along the transverse and longitudinal direction to the weld center, covering all the weld zones as shown in Fig.2b.

2.3 Mechanical testing

Specimens from both weldments were subjected to mechanical testing for finding the effect of joint configuration. The transverse tensile test was carried out in accordance with the ASTME8 Standard Test Methods for Tension Testing of Metallic Materials. The testing was conducted at room temperature on a 100-ton universal testing machine with a constant strain rate of $0.1s^{-1}$. The weldment was also subjected to microhardness testing. Vickers microhardness testing was carried out on a flat polished surface with a load of 1kg and dwell time of 13s as per ASTM:E- 384-11 Standard Test Method for Micro-indentation Hardness of Materials. The Charpy impact test was performed at room temperature as per ASTM E23 Standard Test Methods for Notched Bar Impact Testing of Metallic Materials to calculate the toughness values of the weldjoints.

The fatigue testing was carried out using specimens with across-section of 30.48 x 31.75 mm^2, having a notch and holes for clamping. The fatigue specimens were polished to remove the surface roughness so that crack does not initiate earlier from the surface. The crack tip opening distance (CTOD) method was used on servo-hydraulic high cycle fatigue (HCF) testing machine (Model no: UT-01-0025) as per ASTM E647-15e1 Standard Test Method for Measurement of Fatigue Crack Growth Rates. The specimens were subjected to a load of 6 kN and 0.2 stress ratio (R) at room temperature for a crack length of 6.25 mm. The fractured surfaces of the impact and fatigue specimens were studied for fractographic details using a scanning electron microscope (SEM).

3. Results

3.1 Microstructural observations

The specimens extracted from both the weld joints were subjected to microscopic examination. The test was performed using a precision metallurgical microscope. The specimens were prepared using an automatic electrolyting polishing machine. The etched specimens for V-joint and U-joint are shown in Fig.3 depicting different weldpasses. The microstructure of the root, weldmetal, and HAZ of the joints are shown in Fig.4(a)-(f). Primarily, DSS welds solidify in fully ferritic (δ) mode, forming grain boundary austenite (GBA) at first from δ-ferrite, followed by Widmanstatten austenite (WA) and intragranular austenite (IGA) (Leone and Kerr,1982). All of these forms of austenite can be seen in the microstructure of both welds. The root of the welds (Fig. 4(a) and (b)) contains GBA, WA, IGA as well as secondary austenite (γ_2),which may be formed due to reheating in a multi-pass TIG welding. It is observed from Table 2 that the average heat input to the V-joint is 0.67*kJ/mm,* whereas it is 0.55*kJ/mm* to the U-joint. The approximate values of the cooling rate were 29 K/min for V-joint and 35 K/min for U-joint, confirming that the lower value of heat input results in a higher cooling rate in the steel weldment stated by Arya et al. (2018). The higher cooling rate and reheating in the root of the U-joint lead to the formation of columnar and coarse grains, respectively (Chen et al., 2009). The distribution of the various morphologies of austenite is found to be different in the weld metals of joints (Fig. 4(c) and (d)). The geometry of the V-joint has a sharp converging shape to the root compared to the U-joint. The input heat to the V-joint concentrates whereas, in the U-joint, it spreads over a larger width. Due to this, the V-joint contains a higher amount of IGA than the U-joint due to higher heat input (Geng et al., 2015). Further, the shape of the V-joint led the weld metal to reheat a number of times and nucleate the intragranular austenite from the ferrite grains. These IGA transforms into secondary austenite (γ_2) in the root region of the multi-pass weld due to reheating (Shinetal., 2012).

The weldmetal (WM), the fusion boundary (FB), the heat affected zone (HAZ), and the base metal (BM) are differentiated and shown in Fig. 4(e) and (f). The coarsening of ferrite grains is observed in the HAZ of the V-joint, whereas the HAZ of the U-joint contains the finer ferrite grains. The heat dissipation characteristics (i.e., cooling rate) primarily affect the microstructure of the HAZ in the welds. The fine structure in the HAZ can be attributed to the relatively high cooling rate in the case of U-joint as the high cooling rate reduces the time for the grains to grow (Kumar et al., 2014; Giorjão et al., 2019). It can be seen in Fig.4(e) and Fig. 4(f) that the regular elongated grains in the base metal (BM) gradually turn into the irregular morphologies of ferrite and austenite at the boundary of BM and HAZ in both the weldments. It is known that the increase in heat input and decreasing cooling rate results in an increased area for the HAZ (Kumar et al.,2014; Unnikrishnan et al., 2014; Gupta et al., 2018), and in confirmation of these observations, it is observed that the width of the HAZ for the V-joint is more than that of U-joint.

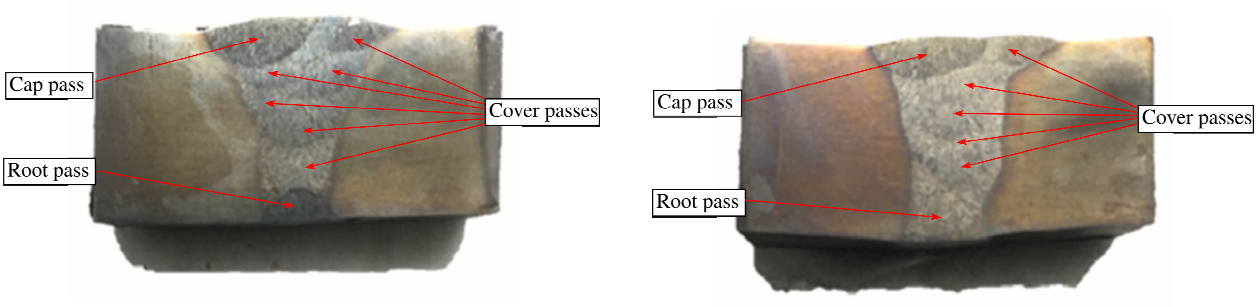

(a) (b)

Figure 3. Macrostructure of the welds joint (a) V-joint, (b) U-joint

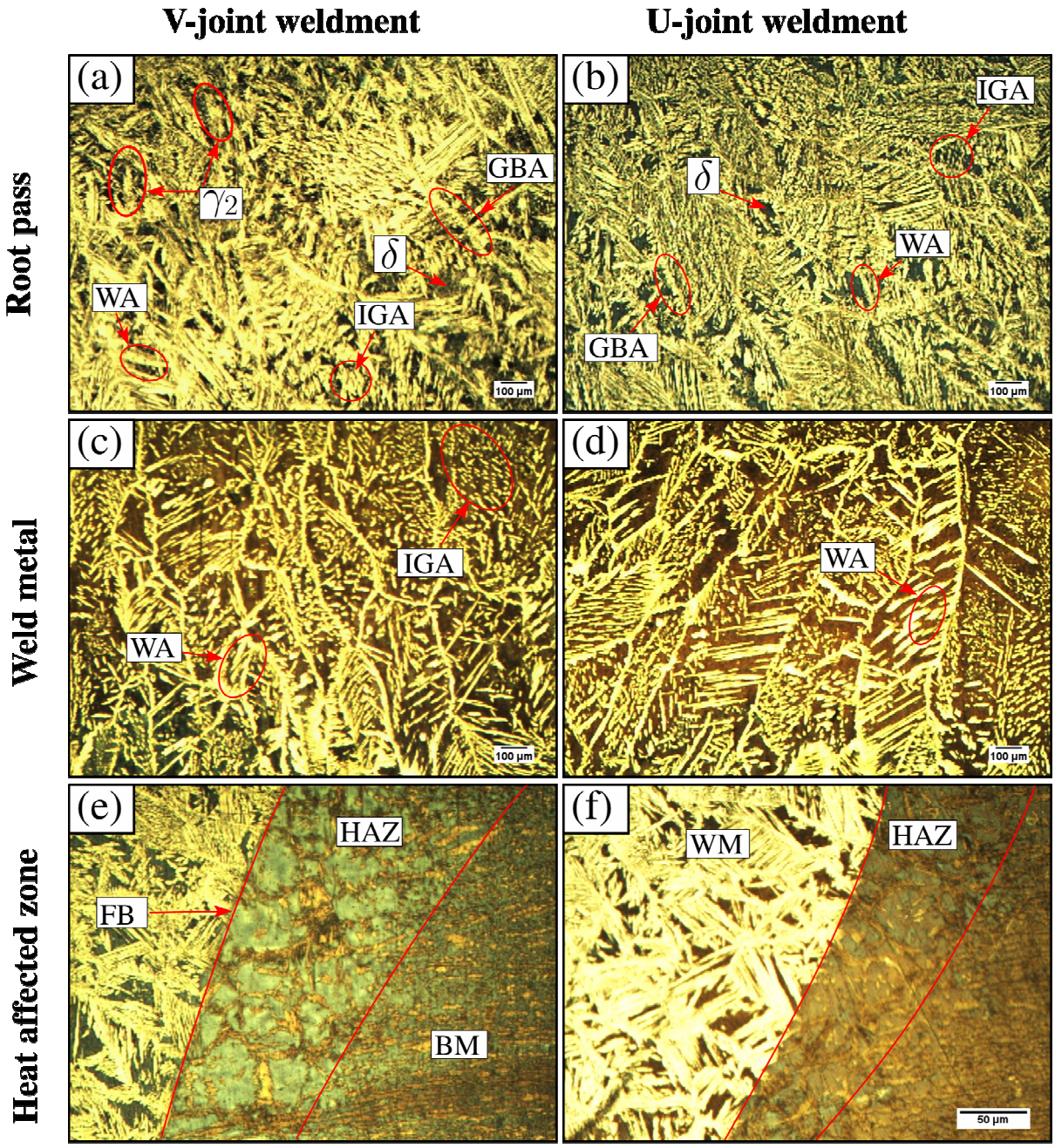

Figure 4. Optical micrographs of the root pass, weld center, and HAZ of V and U-joint, showing δ-ferrite and different morphologies of γ-austenite (GBA, WA, and secondary austenite (γ_2) in different regions of the weld.

3.2 Ferrite fraction study

The ferrite content in the welds was measured along the transverse and longitudinal directional to theweldcenterline.The ferrite measurement was performed using HELMUT Fischer GMBH+CO KG ferritosopeusing the"magnetic induction method" calibrated according to AWS A4.2-91. It is found that the base metal consists of 51.2% ferrite showing the typical phase balance in the microstructure of DSS 2205. A considerable variation in the ferrite contents of both welds is observed when measured along the transverse direction (Fig5a). The weldmetal of the U-joint contains more ferrite volume than that of the V-joint. The higher content of the ferrite phase in the U-joint can be due to a higher cooling rate resulting from lower heat input (Mohammed et al.,2017). The higher cooling rate suppresses the formation of austenite, resulting in more ferrite volume in the weld (Leone and Kerr,1982; Sadeghian et al., 2014). Further, Liao (2018) found that the ferrite content increases in DSS with the

increase in cooling rates. The ferrite content in the HAZ for U-joint is found to be 64% compared to V-joint, which shows around 58%. The maximum ferrite fraction is found at the weld center of the U-joint (65.8%), showing a significant disturbance in the phase balance at the center, whereas V-joint contains 58.3% ferrite at the same location.

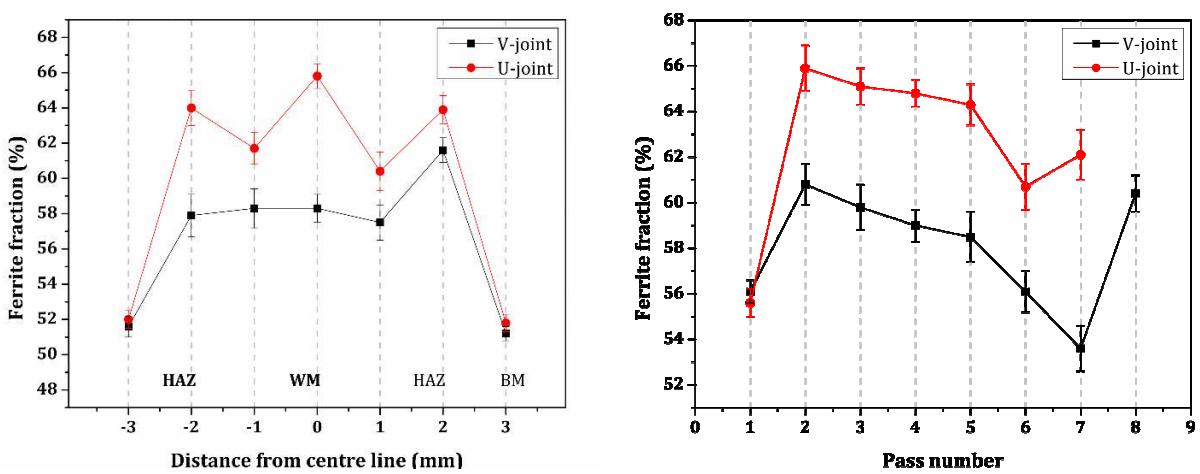

(a) (b)

Figure 5. The variation of ferrite fraction measured along, (a) transverse direction, (b) longitudinal direction

The ferrite content was also measured along the longitudinal direction of the weld. The trend of the ferrite content is similar in both welds, but the U-joint is found to be enriched in the ferrite phase (Fig. 5b). The joint design influences the dilution of the filler metal into the weld metal and the base metal (Vahmanet al.,2020). The alloying elements of the filler metal get diluted into the basemetal as well as into the previous pass of a multi-pass weld (Varbai et al., 2019). The subsequent pass increases the Ni content of the previous weldpass and thus, formed more austenite (Hosseini et al., 2020). The austenite content also increased as the number of welds passes increased (Putz et al., 2019). As the V-joint involved more number of passes, there may be more addition of Ni, and thus the austenite content was more in V-joint as compared to the U-joint. The secondary austenite (γ_2) also formed in the V-joint due to reheating, as is evident from micrographs, which further resulted in the increased austenite content, thus reducing the ferrite fraction in the V-joint. The root pass melted more parent metal as compared to the subsequent passes; therefore, the root of the welds is found to be enriched in ferrite. Due to reheating and addition of Ni in the following passes from the filler metal, the ferrite fraction decreases. The cap pass is found to be enriched with ferrite as it was not reheated by any subsequent pass.

Table 3: Impact and the tensile response of the base metal and welded joints

Specimen	YS (MPa)	UTS (MPa)	Elong. (%)	Strength ratio (YS/UTS)	Toughness (J/cm^2)
BM	480	657	24.2	0.73	215.4
V-joint	617	755	25.9	0.81	255
U-joint	557	766	28.6	0.72	270

3.3 Microhardness investigation

Microhardnes studies were carried out along the transverse and longitudinal directional to the weld center line in different zones of both welds (Fig. 2b). The test was performed using a 2 kg Shimadzu (Asia Pacific) make Micro Vickers hardness testing machine. The spatial location and plan for the microhardness investigation are the same as for the ferrite studies. The microhardness distribution along the transverse direction is presented in Fig.6.The base metal exhibited a microhardnessvalueof243HV.The microhardness of both the welds was higher as compared to the base metal. Across the weld, the U-joint depicts higher microhardness values than the V-joint. At the center of the weld, the microhardness of the U-joint was found to be 18% more than that of the V-joint. The maximum value of microhardness was recorded in the HAZ for the U-joint (359 HV), which was nearly 32% higher as compared to the microhardness of the HAZ of the V-joint. The higher microhardness values of the U-joint can be associated with the higher volume of the δ-ferrite present in the weldmetal of the U-joint (Hosseini et al., 2018). There heating and slower cooling rate of the V-joint during solidification leads to lower ferrite content and higher austenite content in the weld, which decreases the microhardness of the weld (Leone and Kerr, 1982).The V-joint showed no significant variation in the microhardness when measured along the weld center line. The root pass and cap pass of the V-joint exhibited higher microhardness values than

that of the U-joint. The presence of secondary austenite (γ_2) can be attributed to this increased microhardness value at the root of the V-joint (Sieurin andSandström, 2006; Jebaraj andAjaykumar, 2013; Jebaraj et al., 2018).

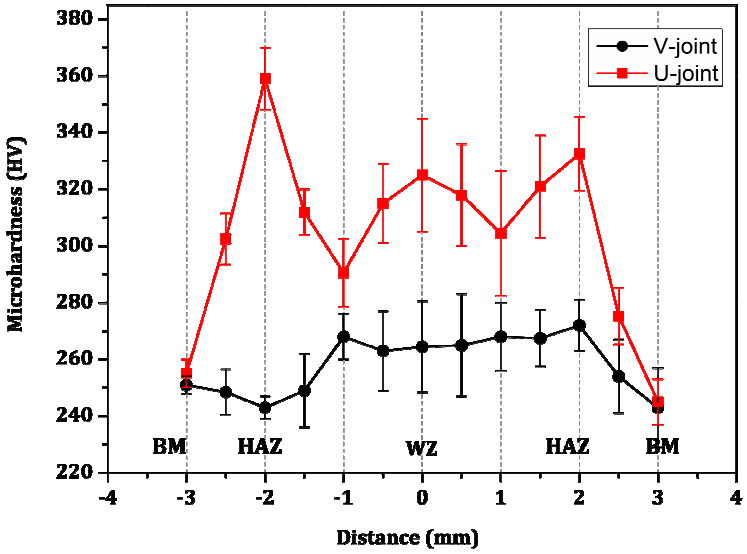

Figure 6. Microhardness variation in the welds along the transverse direction

3.4 Tensile strength study

The tensile properties of the welds, such as yield strength (YS), ultimate tensile strength (UTS), elongation (%), and joint efficiency, were evaluated and are listed in Table 3. The base metal of DSS 2205 possesses YS and UTS of 480 and 657MPa,respectively.The tensile test was performed using Tinius Olsen make 100-tonuniversal testing machine. The Y Sand UTS values for both joints are higher than that of base metal. It is noticed that the U-joint depicts a lower YS of 557 MPa but a higher UTS value of 766 MPa, which is closer to the V-joint. This result concludes that the deformation started at the lower stress value (557 MPa), but it could not initiate the crack as easily in the case ofa U-joint due to a higher UTS (766MPa) and high strain hardening rate.

The fracture location in both joints was found to be at the base metal region during tensile testing. This observation is in confirmation to Giorjão et al. (2019) regarding the failure in lower hardness sites. This fact indicates that 100% joint efficiency is achieved for bothjoints, and supports a good quality of the welded joints. In the fractured specimens, the formation of shear-lip was observed at the end of the crack, indicating the ductile fashion of the fracture. The maximum elongation of 28.6%is observed in the case of the U-joint, although the UTS value is closer to that of the V-joint. The higher elongation of the U-joint is due to the presence of finer grains in comparison to the V-joint, indicating that the stress carrying ability of the U-joint is more than the basemetal and V-joint.

3.5 Impact toughness study

In the present work, the specimen obtained from both the weld joints are subjected to impact testing. The test was performed using a pendulum-type impact testing machine with a maximum capacity of 350*J*. The base metal exhibited a toughness value of 215.4 *J* at room temperature. It is found that the weld metal of both of the joints showed higher toughness values than that of the basemetal. The V-joint depicted the impact toughness of 255 *J* throughout the weld center. The U-joint allowed the weld to absorb more energy resulting in higher toughness (270 *J*) value as compared to V-joint. The higher heat input and slower cooling lead to a coarse-grained structure in the V-joint (Kordatos et al., 2001; Arya et al.,2018; Sun et al.,2016). The lower toughness of the V-joint may be due to the coarsening of the grains. As the dislocation movement in the larger grains is more and resistance to crack propagation is less due to the absence of the grain boundaries, the impact toughness is lower than the U-joint (Songetal.,2016). Further, it is found from Fig.5a that the ferrite content in the U-joint is lower in comparison to V-joint. The higher ferrite content results in a reduction in impact strength (Mouraetal., 2008; Rahmani et al., 2014).

3.6 Fatigue behavior study

The results from the CTOD testing are presented in the form of plots viz. crack length (*a*) vs. no. of cycles (*N*) and fatigue crack growth rate (*da/dN*) vs. stress intensity factor range (ΔK), as shown in Fig.7. The test was performed using 25 kN servo-hydraulic high cycle fatigue testing machine. For the same crack propagation length, the U-joint and V-joint withstood for 64,270 and 55,914 fatigue cycles, respectively. This indicates higher fatigue resistance for the U-joint (in terms of the number of cycles) as compared to the V-joint as well as the base metal (50, 260 cycles). Reyes-Hernández et al. (2017) reported that an increase in the austenite content causes a reduction in fatigue resistance. The increase in the austenite concentration in the weld joint, is at

the expense of its resistance to fatigue loading. The lower value of fatigue resistance is observed for the V-joint, and this observation is in confirmation with the observation reported by Reyes-Hernández et al. (2017), Başyiğit and Kurt (2018), and Ming et al. (2020). The crack propagation rate in U-joint is found to be consistently lower than that of V-joint (Fig. 7b). The crack path and "Fatigue Crack Growth in Reliability (FCGR)" primarily depends upon the grain size in the microstructure. A rough surface produced by the fracture of coarse grain in base metal and weldmetal can withstand a higher number of fatigue cycles and deflect the crack to a tortuous path resulting in reduced FCGR, as pointed out by Kusko et al. (2004). An increasing trend in the fatigue crack growth rate is found with an increase in the value of ΔK for both joints. For the maximum value of ΔK(31.5 $MPa\sqrt{}$), the FCGR (da/dN) for V-joint and U-joint is $2.8e^{-4}$ and $2.58e^{-4}$ $mm/cycle$ respectively. Overall, the weld made with U-joint depicted a lower crack propagation rate as compared to the weld with V-joint, thereby indicating better fatigue performance.

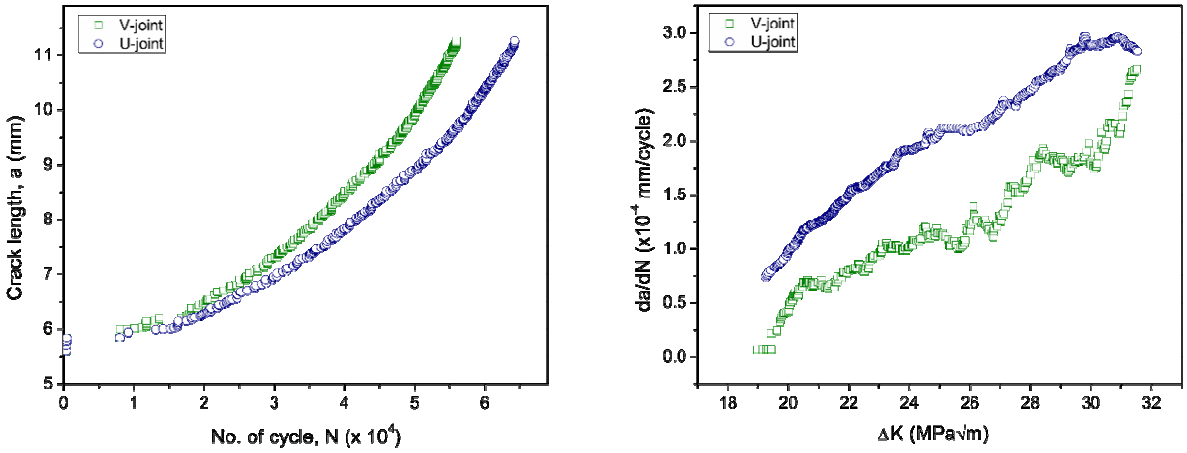

(a) (b)

Figure 7. FCGR results show plots between (a) crack size and the number of cycles, (b) crack

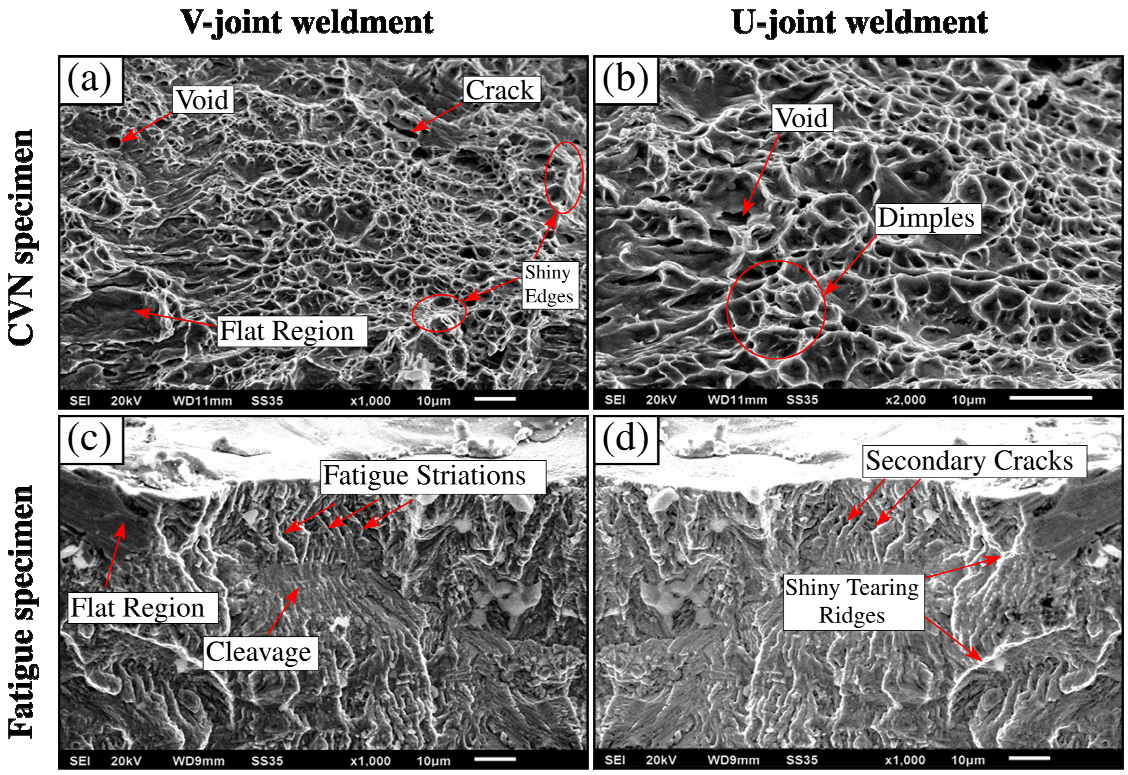

Figure 8. SEM images of the fractured surface for V-joint and U-joint specimens, fractured by CVN and fatigue testing, show various features like voids, dimples, shiny ridges on the fracture surface, and fatigue striation marks, cleavage, and tearing ridges.

3.7 Fractographic investigation

The fracture surface of the specimen subjected to the impact test is analyzed. The test was performed using a scanning electronmicroscope (SEM) available at IIT Ropar. The SEM micrographs for the fractured surface of CVN samples obtained from V-joint and U-joint are shown in Fig. 8(a) and (b). The V-joint CVN fractograph comprises voids, dimples, and shiny ductile regions, indicating the ductile mode of fracture. Unstable cracks, as well as some flat featureless areas, are also found somewhere which dominates the ductile features, provoking the weld to fail in a brittle fashion in those regions absorbing the impact energy of 255 *J*. The fracture surface of the impact sample of the U-joint weld is found to be rich in dimples and voids, which shows the elongated ridges, shiny ductile fields, and deeper voids, indicating a pure ductile fracture of the weld. Unlike the V-joint fracture surface, the flat featureless regions and cracks are not found on the fracture surface of the U-joint. Figures 8(c) and (d) show the fractograph of the fatigue fractured surface of the V-joint and U-joint, respectively. Fatigue striation marks arranged in the bands can be seen clearly, indicating the crack growth for each load cycle and showing the presence of high-intensity cyclic stresses. Cleavage and flat-like features are also observed on the surface marking the brittle zone that might be due to the inclusion of particles. These defects, when observed in front of a crack-tip, a driving force is experienced by the crack facilitating further propagation of the crack and increasing the crack growth rate (da/dN) in proportion to ΔK (Chen et al., 2015). The micrograph shows some secondary cracks deeper beneath the fatigue striations, acting in a ductile fashion. It might be thought that the tip of the primary crack was firmly blunt, which slowed down the crack propagation, but under the influence of high stresses, these secondary cracks nucleated in the vicinity of the primary crack and triggered the same for further propagation.

4. Conclusions

The present work reports the effect of joint design, viz. V-joint and U-joint, on the GTAW weldment for SAF2205 Duplex stainless steel. The joint design is a vital factor for SAF2205 duplex stainless steel (DSS) weld. The cross-section and dimensions for both the joints are judiciously designed to have approximately the same volume. The effect of such a joint design is studied for the metallurgical and mechanical behavior of the weldment in the selected material. Further, the effect of heat input vis-à-vis cooling rate may be investigated as a future extension of the work. In view of the present investigation, the following conclusions are drawn:

- Microstructural studies revealed different morphology of austenite viz. GBA, WA, IGA as well as secondary austenite (γ_2) into the matrix of ferrite in both of the welded joints. A difference in the grain size of HAZ is observed in both joints, showing the influence of the joint design on the heat dissipation characteristics of the weld. The $\alpha-\gamma$ ratio of welds increases due to an increase in ferrite content during the cooling cycle of welding. Locally, the weld metal and HAZ of the U-joint are found to be enriched with ferrite phase as compared to V-joint.
- The average microhardness in weldment with a U-joint was higher than that of a V-joint due to the higher ferrite fraction of the U-groove weld. The impact toughness of both joints is higher than the base metal. The U-joint with the same weld metal volume demonstrated 270 J/cm^2, 25% higher than the BM and 6% higher than the V-joint.
- The tensile specimens of both joints failed from the base metal, showing a 100% joint efficiency of the welds.
- The fatigue life of the U-joint is approximately 15% higher than the V-joint for the same extension incrack length due to the lower austenite fraction in the U-joint. The fatigue crack propagation rate in the U-joint is also found to be lower than in the V-joint.
- The fractured surfaces of the impact test revealed voids, dimples, and tearing ridges for both joints, indicating the ductile failure of the welds. The surfaces of the failed samples under fatigue testing consisted of fatigue striations and shiny ridges, but some secondary cracks are found in the case of U-joint, which supports the higher resistance of the weld to the fatigue loading.

Acknowledgment

The authors acknowledge the Department of Mechanical Engineering, IIT Ropar, and the Department of Mechanical Engineering, SLIET Longowal for allowing using of various testing facilities.

References

Arya, H.K., Singh, K., and Saxena, R.K., 2018, Effect of weld cooling rates on mechanical and metallurgical properties of submerged arc welded pressure vessel steel, *Journal of Pressure Vessel Technology*, Vol. 140, No.4, Article 041406. https://doi.org/10.1115/1.4040274

AWS,2004,Welding Handbook, Vol. II - Welding Processes Part I, 9th Edition, American Welding Society.

Badji, R., Bouabdallah, M., Bacroix, B., Kahloun, C., Belkessa, B., and Maza, H., 2008, Phase transformation and mechanical behavior in annealed 2205 duplex stainless steel welds, *Materials Characterization*, Vol. 59, No. 4, pp. 447–453. https://doi.org/10.1016/j.matchar.2007.03.004

Basyigit, A.B. and Kurt, A., 2018, The effects of nitrogen gas on microstructural and mechanical properties of TIG welded S32205 duplex stainless steel, *Metals*, Vol. 8, No. 4, pp. 226. https://doi.org/10.3390/met8040226

Chen, W., Xue, F., Tian, Y., Yu, D., Yu, W., Chen, X., 2015, Effect of thermal aging on the low cycle fatigue behavior of Z3CN20. 09M cast duplex stainless steel, *Materials Science and Engineering: A*, Vol. 646, pp. 263–271. https://doi.org/10.1016/j.msea.2015.08.070

Chen, Y., Chen, S., and Li, L., 2009, Effects of heat input on microstructure and mechanical property of Al/Ti joints by rectangular spot laser welding-brazing method, *The International Journal of Advanced Manufacturing Technology*, Vol. 44, No. 3-4, pp. 265. https://doi.org/10.1007/s00170-008-1837-2

Koussy, M.El, El Mahallawi, I., Khalifa, W., Al Dawood, M., and Bueckins, M., 2004, Effects of thermal aging on microstructure and mechanical properties of duplex stainless steel weldments, *Materials Science and Technology*, Vol. 20, No. 3, pp. 375–381. https://doi.org/10.1179/174328413X13789824293821

Geng, S., Sun, J., Guo, L., and Wang, H., 2015, Evolution of microstructure and corrosion behavior in 2205 duplex stainless steel GTA-welding joint, *Journal of Manufacturing Processes*, Vol. 19, pp. 32–37. https://doi.org/10.1016/j.jmapro.2015.03.009

Giorjao, R.A.R., Pereira, V.F., Terada, M., da Fonseca, E.B., Marinho, R.R., Garcia, D.M., and Tschiptschin, A.P., 2019, Microstructure and mechanical properties of friction stir welded 8 mm pipe SAF 2507 super duplex stainless steel, *Journal of Materials Research and Technology*, Vol. 8, No. 1, pp. 243–249. https://doi.org/10.1016/j.jmrt.2018.01.002

Gunn, R., 1997, Duplex stainless steels: microstructure, properties and applications, Woodhead Publishing.

Gupta, A., Kumar, A., Baskaran, T., Arya, S.B., and Khatirkar, R.K., 2018, Effect of heat input on microstructure and corrosion behavior of duplex stainless steel shielded metal arc welds, *Transactions of the Indian Institute of Metals*, Vol. 71, No. 7, pp. 1595–1606. https://doi.org/10.1007/s12666-018-1294-z

Hosseini, V.A., Hurtig, K., Eyzop, D., Ostberg, A., Janiak, P., and Karlsson, L., 2018a, Ferrite content measurement in super duplex stainless steel welds, *Welding in the World*, Vol. 63, pp. 551–563. https://doi.org/10.1007/s40194-018-00681-1

Hosseini, V.A., Karlsson, L., Engelberg, D., and Wessman, S., 2018b, Time-Temperature precipitation and property diagrams for super duplex stainless steel weld metals, *Welding in the World*, Vol. 62, No. 3, pp. 517–533. https://doi.org/10.1007/s40194-018-0548-z

Hosseini, V.A., Hurtig, K., and Karlsson, L., 2020, Bead by bead study of a multi-pass shielded metal arc-welded super-duplex stainless steel, *Welding in the World*, Vol. 64, No. 2, pp. 283–299. https://doi.org/10.1007/s40194-019-00829-7

Jang, G., Kim, H., and Kang, S., 2001, The effects of root opening on mechanical properties, deformation, and residual stress of weldments, *Welding Journal Research Supplement*, Vol. 80, No. 3, pp. 80–89.

Jebaraj, A.V. and Ajaykumar, L., 2013, Influence of microstructural changes on impact toughness of weldment and base metal of duplex stainless steel AISI 2205 for low-temperature applications, *Procedia Engineering*, Vol. 64, pp. 456–466. https://doi.org/10.1016/j.proeng.2013.09.119

Jebaraj, A.V., Ajaykumar, L., Deepak, C., and Aditya, K., 2017, Weldability, machinability, and surfacing of commercial duplex stainless steel AISI-2205 for marine applications: A recent review, *Journal of Advanced Research*, Vol. 8, No. 3, pp. 183-199. https://doi.org/10.1016/j.jare.2017.01.002

Jebaraj, A.V., Kumar, T.S., and Manikandan, M., 2018, Investigation of structure-property relationship of the dissimilar weld between austenitic stainless steel 316L and duplex stainless steel 2205, *Transactions of the Indian Institute of Metals*, Vol. 71, No. 10, pp. 2593–2604. https://doi.org/10.1007/s12666-018-1392-y

Kordatos, J., Fourlaris, G., and Papadimitriou, G., 2001, The effect of cooling rate on the mechanical and corrosion properties of SAF 2205 (UNS 31803) duplex stainless steel welds, Scripta materialia, Vol. 44(3), pp. 401–408. https://doi.org/10.1016/S1359-6462(00)00613-8

Kumar, R., Arya, H.K., and Saxena, R.K., 2014a, Effect of cooling rate on microstructure of SAW welded mild steel plate (grade C-25 as per IS 1570), *International Journal of Modern Engineering Research*, Vol. 4, No. 1, pp. 222-228.

Kumar, R., Arya, H.K., and Saxena, R.K., 2014b, Experimental determination of cooling rate and its effect on microhardness in submerged arc welding of mild steel plate (grade C-25 as per IS 1570), *Journal of Material Science & Engineering*, Vol. 3, No. 2, pp. 1–4. https://doi.org/10.4172/2169-0022.1000138

Kusko, C., Dupont, J., and Marder, A., 2004, The influence of microstructure on fatigue crack propagation behavior of stainless-steel welds, *Welding Journal*, Vol. 83, No. 1, pp. 6–14.

Leonard, A., Gunn, R., and Gooch, T., 2000, Hydrogen cracking of ferritic-austenitic stainless steel weld metal, Presented at '*Stainless Steel World Duplex America 2000*' Conference, 29 February - 1 March 2000.

Leone, G. and Kerr, H., 1982, The ferrite to austenite transformation in stainless steels, *Welding Journal*, Vol. 61, No. 1, pp. 13S–21S.

Liao, L., 2018, Ferrite percentage prediction of duplex stainless steels as a function of cooling rates, Ph.D. thesis, *Materials Science and Engineering Department*, Iowa State University.

Lin, K., Shi, H.Q., Ma, L.Q., and Ding, Y., 2012, The analysis and research of secondary phases generated during isothermal aging of duplex stainless steels, *Applied Mechanics and Materials*, Vol. 193, pp. 411–417. https://doi.org/10.4028/www.scientific.net/AMM.193-194.411

Ling, K.-H., Fuh, Y.-K., Wu, K.-L., Kuo, T.-C., and Huang, C.-Y., 2015, Groove configurations of a flux-cored arc welding process used in critical structures of precision mechanical pressesmechanical and metallurgical studies, *The International Journal of Advanced Manufacturing Technology*, Vol. 78, No. 9-12, pp. 1905–1916. https://doi.org/10.1007/s00170-014-6766-7

Luo, J., Dong, Y., Li, L., and Wang, X., 2014, Microstructure of 2205 duplex stainless steel joint in submerged arc welding by post weld heat treatment, *Journal of Manufacturing Processes*, Vol. 16, No. 1, pp. 144–148. https://doi.org/10.1016/j.jmapro.2013.06.013

Ming, Z., Wang, K., Liu, Z., Wang, W., and Wang, Y., 2020, Effect of the cooling rate on the microstructure and mechanical properties of high nitrogen stainless steel weld metals, *China Welding*, Vol. 29, pp. 48.

Mohammed, G.R., Ishak, M., Aqida, S.N., and Abdulhadi, H. A., 2017, Effects of heat input on microstructure, corrosion and mechanical characteristics of welded austenitic and duplex stainless steels: A review, *Metals*, Vol. 7, No. 2, pp. 39. https://doi.org/10.3390/met7020039

Moura, V., Lima, L., Pardal, J., Kina, A., Corte, R., and Tavares, S., 2008, Influence of microstructure on the corrosion resistance of the duplex stainless steel UNSS31803, *Materials Characterization*, Vol. 59, No. 8, pp. 1127–1132. https://doi.org/10.1016/j.matchar.2007.09.002

Munez, C., Utrilla, M., Urena, A., and Otero, E., 2010, Influence of the filler material on pitting corrosion in welded duplex stainless steel 2205, *Welding International*, Vol. 24, No. 2, pp. 105–110. https://doi.org/10.1080/09507110902843362

Muthupandi, V., Srinivasan, P.B., Seshadri, S., and Sundaresan, S., 2003, Effect of weld metal chemistry and heat input on the structure and properties of duplex stainless steel welds, *Materials Science and Engineering: A*, Vol. 358, No. 1-2, pp. 9–16. https://doi.org/10.1016/S0921-5093(03)00077-7

Paulraj, P. and Garg, R., 2016, Effect of welding parameters on pitting behavior of GTAW of DSS and super DSS weldments, *Engineering Science and Technology, an International Journal*, Vol. 19, No. 2, pp. 1076–1083. https://doi.org/10.1016/j.jestch.2016.01.013

Putz, A., Althuber, M., Zelic, A., Westin, E., Willidal, T., and Enzinger, N., 2019, Methods for the measurement of ferrite content in multipass duplex stainless-steel welds, *Welding in the World*, Vol. 63, No. 4, pp. 1075–1086. https://doi.org/10.1007/s40194-019-00721-4

Rahmani, M., Eghlimi, A., and Shamanian, M., 2014, Evaluation of microstructure and mechanical properties in dissimilar austenitic/super duplex stainless steel joint, *Journal of Materials Engineering and Performance*, Vol. 23, No. 10, pp. 3745–3753. https://doi.org/10.1007/s11665-014-1136-z

Reyes-Hernandez, D., Manzano-Ramırez, A., Encinas, A., Sanchez-Cabrera, V., de Jesus, A. M., Garcıa-Garcıa, R., Orozco, G., and Olivares-Ramırez, J., 2017, Addition of nitrogen to GTAW welding duplex steel 2205 and its effect on fatigue strength and corrosion, *Fuel*, Vol. 198, pp. 165–169. https://doi.org/10.1016/j.fuel.2017.01.008

Sadeghian, M., Shamanian, M., and Shafyei, A., 2014, Effect of heat input on microstructure and mechanical properties of dissimilar joints between super duplex stainless steel and high strength low alloy steel, *Materials & Design*, Vol. 60, pp. 678–684. https://doi.org/10.1016/j.matdes.2014.03.057

Sharma, V. and Shahi, A., 2014, Effect of groove design on mechanical and metallurgical properties of quenched and tempered low alloy abrasion resistant steel welded joints, *Materials & Design*, Vol. 53, pp. 727–736. https://doi.org/10.1016/j.matdes.2013.07.043

Shin, Y.-T., Shin, H.-S., and Lee, H.-W., 2012, Effects of heat input on pitting corrosion in super duplex stainless steel weld metals, *Metals and Materials International*, Vol. 18, No. 6, pp. 1037–1040. https://doi.org/10.1007/s12540-012-6017-0

Sieurin, H. and Sandstrom, R., 2006, Austenite reformation in the heat-affected zone of duplex stainless steel 2205, *Materials Science and Engineering: A*, Vol. 418, No. 1-2, pp. 250–256. https://doi.org/10.1016/j.msea.2005.11.025

Song, T., Jiang, X., Shao, Z., Mo, D., Zhu, D., and Zhu, M., 2016, The interfacial microstructure and mechanical properties of diffusion-bonded joints of 316L stainless steel and the 4j29 Kovar alloy using nickel as an interlayer, Metals, Vol. 6(11), pp. 263.

Sun, Y., Wu, X., Wu, X., Li, J., and Jiang, Y., 2016, Influence of multi-pass welding on the microstructure evolution and corrosion resistance of a super duplex stainless steel, *International Journal of Electrochemical Science*, Vol. 11, No. 11, pp. 9666–9675. https://doi.org/10.20964/2016.11.28

Unnikrishnan, R., Idury, K.S., Ismail, T., Bhadauria, A., Shekhawat, S., Khatirkar, R.K., and Sapate, S.G., 2014, Effect of heat input on the microstructure, residual stresses and corrosion resistance of 304l austenitic stainless-steel weldments, *Materials Characterization*, Vol. 93, pp. 10–23. https://doi.org/10.1016/j.matchar.2014.03.013

Vahman, M., Shamanian, M., Golozar, M.A., Jalali, A., Sarmadi, M.A., and Kangazian, J., 2020, The effect of welding heat input on the structure-property relationship of a new grade super duplex stainless steel, *Steel Research International*, Vol. 91, No. 1, Article 1900347. https://doi.org/10.1002/srin.201900347

Varbai, B., Adonyi, Y., Baumer, R., Pickle, T., Dobranszky, J., and Majlinger, K., 2019, Weldability of duplex stainless steels-thermal cycle and nitrogen effects, *Welding Journal*, Vol. 98, No. 3, pp. 78–87. https://doi.org/10.29391/2019.98.006

Verma, J. and Taiwade, R.V., 2017, Effect of welding processes and conditions on the microstructure, mechanical properties, and corrosion resistance of duplex stainless steel weldments-a review, *Journal of Manufacturing Processes*, Vol. 25, pp. 134–152. https://doi.org/10.1016/j.jmapro.2016.11.003

Zhang, Z., Jing, H., Xu, L., Han, Y., Zhao, L., and Zhou, C., 2017, Effects of nitrogen in shielding gas on microstructure evolution and localized corrosion behavior of duplex stainless steel welding joint, *Applied Surface Science*, Vol. 404, pp. 110–128. https://doi.org/10.1016/j.apsusc.2017.01.252

Zhang, Z., Wang, Z., Jiang, Y., Tan, H., Han, D., Guo, Y., and Li, J., 2012, Effect of post-weld heat treatment on microstructure evolution and pitting corrosion behavior of UNS S31803 duplex stainless-steel welds, *Corrosion Science*, Vol. 62, pp. 42–50. https://doi.org/10.1016/j.corsci.2012.04.047

Biographical notes

Rajat Dhiman, Sorabh Singhal and Ravindra K. Saxena are of the Department of Mechanical Engineering, Sant Longowal Institute of Engineering and Technology, Longowal-148106, Punjab, India.